Trees
https://doi.org/10.1007/s00468-024-02575-w

ORIGINAL ARTICLE

Mechanism of wetwood formation in silver fir (*Abies alba* Mill.)

Ludovic Martin[1] · **Nicole Brunel-Michac**[1] · **Pierre Conchon**[1] · **Hervé Cochard**[1] · **Eric Badel**[1]

Received: 19 July 2024 / Accepted: 27 September 2024

Abstract

Key message **Hydraulic properties of wetwood differ from normal sapwood: hydraulic conductivity is null and water contained in wetwood is totally trapped. Wetwood could result from a bad healing of dead branches.**

Abstract Wetwood is a common phenomenon in silver fir (*Abies alba* Mill.), posing technical challenges for its industrial use. In this study, we thoroughly characterized the properties of this particular wood, investigating the mechanisms governing its formation and exploring its potential physiological relevance for trees. To address these objectives, we used a wide range of techniques, offering a comprehensive insight into the structure of wetwood at different scales, from cellular to whole-tree. Our results revealed significant variability in moisture distribution in the heartwood of the silver fir trees studied, suggesting the absence of a predefined distribution pattern. The physical properties of wetwood differ from those of sapwood, notably in terms of its hydraulic conductivity, which is null. In addition, our study demonstrated that the anatomical characteristics of wetwood are identical to those of normal dry heartwood, including features such as aspirated tori in bordered pits and the absence of nuclei. These results suggest a normal initial duraminization process followed by a progressive resaturation of the heartwood of silver fir. Taken together, these observations strongly suggest that the water present in wetwood is trapped and unavailable for use by the tree, particularly under conditions of prolonged drought.

Keywords Water accumulation · Hydraulics · Embolism · Physical properties · Physiology

Introduction

Wetwood refers to areas of xylem in standing trees that have abnormally high moisture content (MC) compared to the surrounding heartwood (Ward and Pong 1980). This phenomenon is common and often considered normal in the inner wood of many tree species, including both hardwoods and conifers (Martin et al. 2021; Moya et al. 2009; Nakada et al. 2003; Ward and Pong 1980). Wetwood can exhibit varying physical characteristics, such as color, odor, and moisture content, which may differ not only between species, but also within a single species. After felling, wetwood areas typically appear darker than both the surrounding dry heartwood and the sapwood on the cross-section (Martin et al. 2021; Moya et al. 2009; Nakada et al. 2003; Ward and Pong 1980).

Unlike sapwood, which typically has a relatively uniform moisture content, wetwood can exhibit significant heterogeneities, with some areas completely saturated with water and others much drier (Coutts and Risbeth 1977; Mackay 1975; Martin et al. 2021; Nakada 2006; Schneider and Zhou 1989). Furthermore, the magnitude of differences in MC can vary across species and studies. For example, in studies on *Abies balsamea* Mill. (Jeremic et al. 2004), *Abies firma* (Nakada 2006), and *Abies concolor* Lindl. (Worrall and Parmeter 1982), the average MC of wetwood was similar to that of sapwood, around 180% of dry weight. In contrast, in a study on *Abies borisii regis* Mattf., the average MC of wetwood was much lower, around 80%, compared to the 140% measured in the sapwood (Passialis and Tsoumis 1984). Finally, wetwood can also have much higher MC than sapwood, as in the case of *Gmelina arborea*, where the average wetwood MC, measured at 182%, was significantly higher than the 149% measured in the sapwood (Moya et al. 2009).

The occurrence and distribution of wetwood in tree trunks appears to vary across species and studies. Wetwood has

Communicated by A. Nardini .

Ludovic Martin
ludovic.martin@inrae.fr

[1] Université Clermont Auvergne, INRAE, PIAF, 63000 Clermont–Ferrand, France

Published online: 09 October 2024

been observed as a cone shape tapering from the base to the top of tree trunks, narrowing downwards and ending in the roots in some studies (Coutts and Rishbeth 1977; Passialis and Tsoumis 1984); and sometimes as spots or streaks (Coutts and Rishbeth 1977; Martin et al. 2021; Nakada 2006; Ward and Pong 1980). Works on *Cryptomeria japonica* D. Don have shown significant variation in the distribution of water within heartwood, both horizontally and longitudinally, highlighting the absence of a universal pattern of moisture distribution along the stems of heartwood (Nakada et al. 2003).

The physical properties of wetwood may vary depending on the species and the study. Several studies on fir trees have found no correlation between the presence of wetwood and wood density or shrinkage after drying (Jeremic et al. 2004; Passialis and Tsoumis 1984; Wilcox 1968). In some hardwoods, including *Gmelina arborea* and *Quercus* species, wetwood was reported to have higher shrinkage rates and lower densities than the rest of the wood (Moya et al. 2009; Xu et al. 2001). Conversely, wetwood in *Populus* species and *Abies concolor* has been found to have higher density than sapwood or dry heartwood (Ward 1984). Wetwood seems to dry slower than sapwood but at a similar rate to heartwood (Jeremic et al. 2004; Moya et al. 2009; Ward 1985). It is also reported to be much less permeable than sapwood but slightly more permeable than normal heartwood (Schneider and Zhou 1989; Ward 1985).

Several other characteristics of wetwood can be highlighted, including its occurrence even in young trees (Coutts and Rishbeth 1977; Passialis and Tsoumis 1984), and notable variation in its prevalence within tree populations. Indeed, the proportion of trees containing wetwood varies widely among studies, with estimates ranging from 50 to 100% of the trees studied (Jeremic et al. 2004; Martin et al. 2021; Passialis and Tsoumis 1984). This variability may be explained by differences in tree diameter (Martin et al. 2021) or soil type (Lihra et al. 2000; Krause and Cagnon 2006). The presence of wetwood has also been associated with tree growth vigor, with higher levels of wetwood found in fast-growing trees compared to slow-growing ones (Coutts and Rishbeth 1977; Etheridge and Morin 1962).

Depending on the species studied and the research conducted, various external causes leading to the formation of wetwood have been suggested. Reactions to pathogens, such as bacteria, are among the potential factors that have been proposed as potential causes (Bauch et al. 1975; Schink and Ward 1984). However, while some studies have observed more bacteria in wetwood (Etheridge and Morin 1962; Ward and Zeikus 1980), others have found no link between bacteria and wetwood (Jeremic et al. 2004; Krause and Cagnon 2005). Studies have also postulated that the presence of wetwood provides protection against injury and fungi by creating unfavorable conditions for fungal growth (Coleman et al. 1985; Van der Kamp et al. 1979; Worrall and Parmeter 1982). Although several studies have hypothesized that branch breaks and root wounds may be the preferred external access points for water stored in wetwood (Bauch et al. 1975; Krause and Cagnon 2005), others have suggested that sapwood may be the primary source of water in wetwood (Coutts and Rishbeth 1977; Nakada et al. 2019). Finally, despite extensive works, the key factors in the origins of wetwood formation and its physical characteristics remain under debate.

In this study, we explored two hypotheses that could account for the formation of wetwood in silver fir trees (*Abies alba* Mill.): (1) a defect in heartwood formation that leads to continuous water presence in tracheids, or (2) the posterior entry of water into embolized tracheids. We investigated wetwood areas at the tree, tissue, cellular, and cell wall levels to test these hypotheses, including hydraulic traits and anatomical patterns of wetwood compared to normal wood. Finally, given wetwood's high water content, we hypothesized that it could serve as a water reservoir for trees during drought, which could be a great physiological advantage in the context of climate changes. Following this hypothesis, we also investigated the possible hydraulic connection of these water reservoirs with the other functional hydraulic network of the trees.

Materials and methods

Plant material

Silver fir trees (*Abies alba*) were sampled in three different forest plots in Puy-de-Dôme, France. The first two plots, Guery 1 and Guery 2, are located in the domanial forest of Guery in the Sancy (South-West part of Puy-de-Dôme). Guery 1 is a monospecific forest of Silver fir trees situated at 45°37′43″N, 2°48′11″E, ranging between 1110 and 1130 m above sea level, with a 15% slope facing North-East. Guery 2 is a mixed forest of Silver fir and Beech trees located at 45°38′18″N, 2°19′4″E, ranging from 1030 to 1080 m above sea level, with a 55% slope facing West. The trees from both plots were subject to a mean annual temperature of 7.6 °C and a mean annual precipitation of 1148 mm. The third plot, Saint-Germain, is situated in Livradois (South-East part of Puy-de-Dôme). Saint-Germain is a monospecific forest of old Silver fir trees located at 45°29′6″N, 3°31′32″E, on a plateau at 1040 m for one section and at 940 m above sea level for another, with a 30% slope facing North–West. Trees from this plot are subject to a mean annual temperature of 8.9 °C and a mean annual precipitation of 933 mm. Three trees from plot 2 were felled for X-ray scanning measurements, with diameters of approximately 38 cm to fit the dimensions of the X-ray scanner. Two trees from plot 1 and an additional tree from plot 2, which had significant areas of wetwood, were felled to collect samples for conductivity and drying experiments, high-resolution X-ray microtomography, and histological measurements. An additional tree from plot 1 was used for a girdling experiment.

CT scanning of logs

Nine logs from three silver fir trees from plot 2 were subjected to CT scanning in early July 2019. From each tree, three 1.5 m long logs were cut at different heights, specifically at the base of the trunk, the base of the crown, and an intermediate section between these two points (Fig. 2A). The logs were then wrapped in plastic bags and transported to the "SilvaTech" facility (Nancy, France). Each log was scanned using a medical CT scanner (GE BrightSpeed Excel) as shown in Fig. 1A. The image of the transverse section had a spatial resolution of 0.88 mm/pixel, and a slice thickness of 0.625 mm. The X-ray source parameter were fixed at 80 kV and 50 mA, using a helical mode.

Wood hydraulic properties characterization

We used three different techniques to measure and compare the hydraulic properties of sapwood, heartwood, and wetwood. These measurements were conducted on wood samples obtained from three trees, previously selected using an Electrical Resistivity Tomography tool (ERT) for the non-destructive detection of wetwood (as described by Martin et al. 2021), and containing significant areas of wetwood.

The wood's longitudinal conductivity was measured using a Xyl'em device (Xyl'em, Bronkhorst, Montigny-les-Cormeilles, France) on three transversal slices of wood, each 10 cm thick in the longitudinal direction (Cochard et al. 2013). After an initial chainsaw cut, each sample containing the three wood zones of interest (sapwood, dry heartwood, and wetwood) was placed in a water-filled tank (Fig. 2A). Following a new cutting of small areas of a few mm^2 under water with a razor blade, a cork borer with a diameter of 3 mm was inserted into the wood at each measuring point (9 per sample). The needle was connected by a pipe to the Xyl'em device, which delivered water into the sample. The xylem hydraulic conductivity (K) is defined as the mass flow (F, $mmol.s^{-1}$) of water passing through a segment exposed to a gravimetric pressure gradient P/l ($MPa.m^{-1}$), where l is the sample length (m). The unit for K is $mmol.m.s^{-1}.MPa^{-1}$ (Cochard et al. 2013; Sperry et al. 1988). The constancy of the xylem section in the needle allows for a direct comparison of K values across samples.

The vulnerability to cavitation of sapwood and wetwood was measured using a centrifuge technique (Fig. 1C; Cochard et al. 2005). For this experiment, pieces of wood about 1 cm^2 in section and 28 cm long were cut from sapwood (n = 5) and wetwood (n = 10) areas (Fig. 3A, Fig. S1A). In order to reduce the potential damage to the surface conduits, the wood samples were separated as far as possible along the grain. Each xylem segment was installed on the axis of a centrifuge with its ends

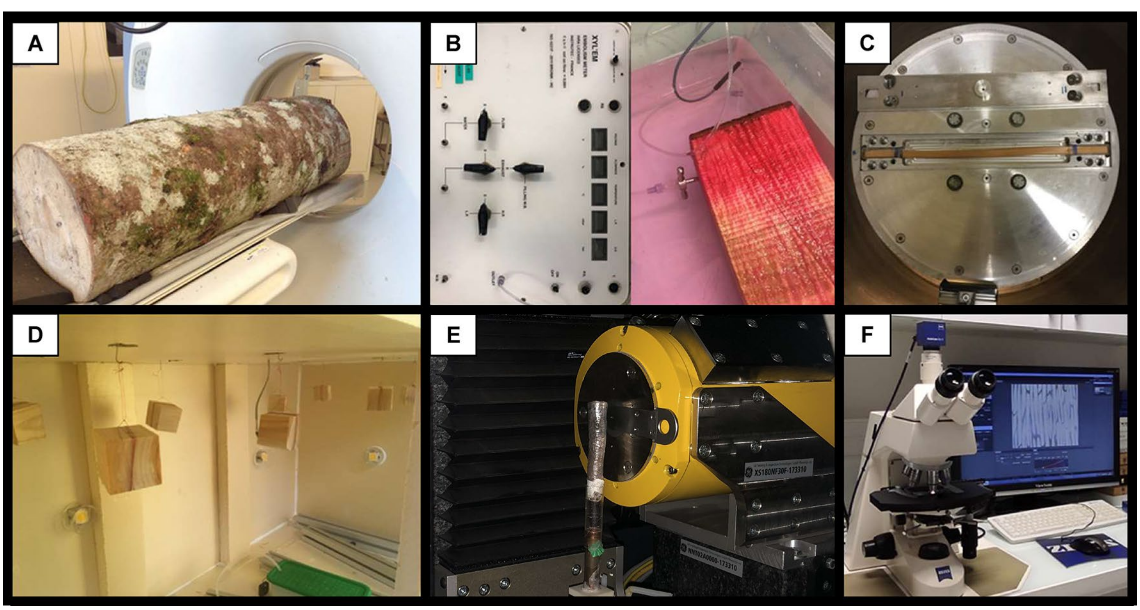

Fig. 1 Photographs presenting the different devices and techniques used for the wetwood investigations. X-ray medical scanner on logs for wetwood mapping at the trunk scale (**A**), Xyl'em device for wood conductivity measurements (**B**), Centrifugation technique for wood water retention measurements (**C**), DroughtBox for wood drying kinetics under controlled conditions (**D**), X-ray microtomography observation (**E**), and histological analysis (**F**)

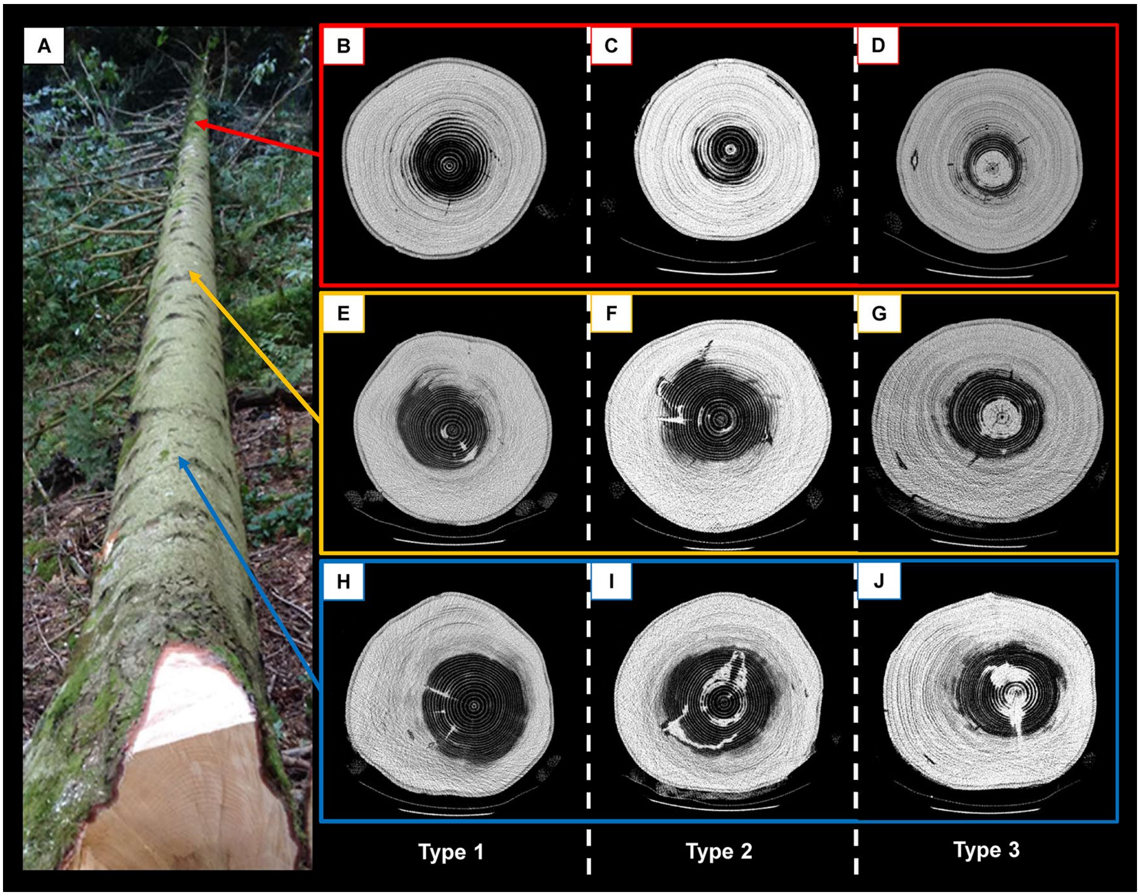

Fig. 2 Spatial distribution of water in a trunk. Cross-section observation by X-ray scanning enlightened the contrast between the water saturated and embolised areas. Three fir trees (Type 1, Type 2 and Type 3) were scanned at 3 different heights: 1 m (**H**, **I**, **J**), 8 m (**E**, **F**, **G**) and 14 m (**B**, **C**, **D**). The arrows indicate the relative positions of the scans in the trunk (**A**). On the nine X-ray scanning images, black areas indicate air-filled tracheids, light grey areas indicate the water-filled tracheids

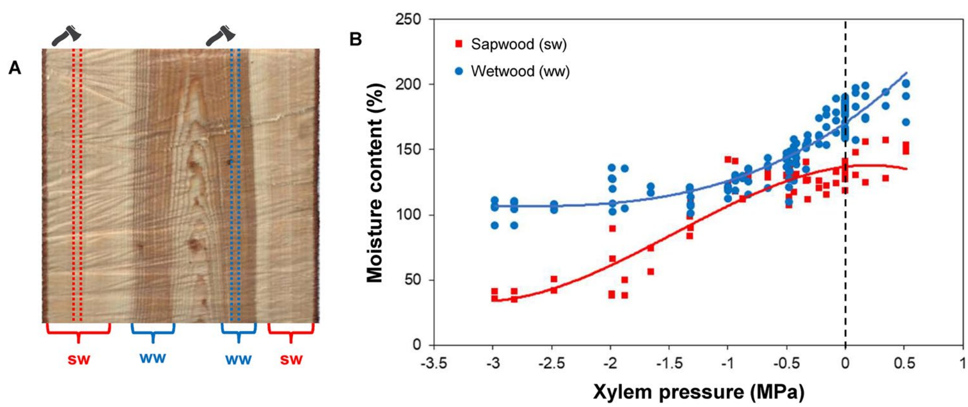

Fig. 3 Water retention curve of sapwood (red) and wetwood (blue) in relation to the negative hydrostatic pressure. Photograph showing the position of 28 cm-long xylem segments cut longitudinally and used for measurements in sapwood (sw) and wetwood (ww) areas (**A**). Each point of the plot represents the moisture content of 2 cm long segment after centrifugation (**B**)

immersed in 1 cm of water contained in two plastic reservoirs and then centrifuged for 1 h. Holes in the reservoir wall maintained the water level constant. This technique involves rotating the sample through its center and using centrifugal force to generate negative pressures (P, MPa) in the sample. Thanks to this method, each part of the sample experiences a local xylem pressure that is evaluated according to its radial position x in the centrifuge as follows:

$$P = -0.25\rho\omega^2\left[R^2 - (R - x)^2\right] \quad (1)$$

where ρ is the density of water (1000 kg m^{-3}), ω is the angular speed (rad s^{-1}), R is the distance (in m) from the axis of rotation to the water surface in the reservoir, and x the position on the sample axis. The xylem pressure is minimum in the middle of the sample and null at the water surface in the cuvettes, and slightly positive at the sample's ends (Cochard et al. 2005). Five different speeds, corresponding to pressures of 0, − 0.5, − 1, − 2, and − 3 MPa, were imposed on one sapwood and two wetwood segments. The gradients of xylem pressures sustained by the samples are presented in Fig. S1B. After centrifugation, each xylem segment was cut into fourteen 2 cm long samples, and their fresh mass (FW) was immediately measured. The samples were then dried for at least 24 h at 104 °C, and their dry mass (DW) was measured to determine their moisture content (MC, Eq. 2).

Drying kinetics of sapwood and wetwood were investigated using cubic samples measuring 5 × 5x5 cm^3. To control the drying direction (longitudinal, radial, or tangential), five out of six faces of each sample were coated with liquid paraffin. The coated samples were then placed in a DroughtBox, a hermetic and insulated chamber made of 40 mm thick polystyrene boards (Billon et al. 2020). The DroughtBox allowed for the control of temperature and humidity within the chamber and real-time monitoring of mass variations of each sample via strain gauges. Samples were attached to strain gauges through holes in the roof board and placed at a constant temperature of 30 °C and humidity of 45% for a duration of 5 days (Fig. 1D).

Direct X-ray microtomography (micro-CT) visualization of embolism at cell level in cores

X-ray micro-CT scans were conducted on radial cores obtained using a 10 mm width increment borer (Haglöf Sweden AB, Lansele, Sweden). The cores were promptly wrapped in parafilm and transported in a cooler to the laboratory where they were trimmed to 100 mm length in the radial direction with a razor blade and coated with liquid paraffin wax to prevent drying during scanning. The cores were then scanned using an X-ray microtomograph (Nanotom 180 XS; GE, Wunstorf, Germany) according to the protocol described by Cochard et al. (2015) (Fig. 1E) using a z-project module in order to automatically scan the long radial core. The micro-CT scan's field of view was set to 10 × 10 × 50 mm (tangential, longitudinal and radial directions respectively), and the X-ray source was adjusted to 60 kV and 240 µA. During each 21 min scan, 1000 images were recorded as the sample was rotated 360°. After 3D reconstruction, the final volumetric image had a spatial resolution of 5.3 × 5.3 × 5.3 μm^3 per voxel. Virtual slices depicting the radial-tangential plane were extracted from the center of each 3D volume using VGStudio Max© software (Volume Graphics, Heidelberg, Germany) to visualize the local embolism at the cellular level.

Histological analysis

To perform histological observations, cubes measuring approximately 1 cm on each side were obtained from sapwood, heartwood, and wetwood. Wood sticks measuring 8 mm in length and 3 × 3 mm in cross-section were re-cut using a razor blade. The samples were then fixed, dehydrated, and gradually infiltrated with white medium-grade LR White resin following the method described by Azri et al. (2009). Thin transversal and tangential sections, 2 µm thick, were prepared using an OmU2 rotary microtome (Reichert, Vienna, Austria) equipped with a Diatome diamond knife (LFG Distribution, Lyon, France). The sections were stained with 0.5% toluidine blue and all images were captured using a Zeiss Axioskop 40 microscope, digital camera, and Zen imaging software system (Zeiss, Jena, Germany).

Tree girdling experiment and local wood moisture content measurements on cores

In early September 2018, a 47 cm diameter tree, from plot 1, with a wetwood zone covering the entire heartwood was selected using an electrical resistivity tomograph (see Martin et al. 2021 for more details). Girdling was performed using a chainsaw by notching the trunk at a height of 50 cm to a depth of 10 cm in order to completely incise the sapwood and stop the flow of sap. Cores were sampled from 1 m above the girdling area on the day of girdling and 10, 90 and 650 days later. We collected wood cores using a 5 mm width increment borer (Haglöf Sweden AB, Lansele, Sweden). After sampling, we cut the cores into 10 cm pieces and placed them immediately in plastic tubes, which we brought to the laboratory in a cooler. We then cut each piece into 10 mm samples and measured its fresh mass (FW) immediately. We dried the samples for at least 24 h at 104 °C and measured their dry mass (DW). We calculated the wood moisture content (MC %) using Eq. (2):

$$MC\% = \frac{FW - DW}{DW} * 100 \tag{2}$$

Infradensity of wood

Infradensity measurements were conducted on 2093 heartwood cylindrical samples, each measuring 10 mm in length and 5 mm in diameter. These samples, which contain either normal heartwood, wetwood, or a combination of both, were collected using a 5 mm width increment borer (Haglöf Sweden AB, Lansele, Sweden) from 58 fir trees within our three forest plots (see Martin et al. 2021 for more details about the sampled trees).

The infradensity ρ_w was evaluated using the following formula:

$$\rho_W = DW/V \tag{3}$$

where DW is the owen-dry mass of the wood and V the volume of the green wood sample.

Table 1 Moisture content (%) and hydraulic conductivity ($mmol.m.s^{-1}.MPa^{-1}$)

	Sapwood	Dry heartwood	Wetwood
Moisture content (%)	144.5 ± 21.1^a	44.9 ± 5.4^b	151.8 ± 23.6^a
Conductivity ($mmol.m.s^{-1}.MPa^{-1}$)	28.6 ± 4^a	0 ± 0^b	0 ± 0^b

Comparison of wetwood, sapwood and dry heartwood

Results

Mapping the wetwood areas in the trunk

The spatial distribution of wetwood in fir tree trunks was investigated through X-ray scanning of 1 m logs collected at three different heights (Fig. 2A) from three trees preselected using electrical resistance tomography (ERT). These trees were chosen based on three distinct ER profiles, as described in Martin et al. (2021). Type 1 refers to heartwood without wetwood. Type 2 refers to heterogeneous heartwood containing wetwood patches, and Type 3 refers to an almost homogeneous central wetwood area. Our findings indicated that trees with Type 1 profiles, i.e., little to no wetwood at the trunk base, also lacked significant wetwood areas elsewhere in the trunk (Fig. 2B, E, H). For Type 3 trees (Fig. 2J), the central wetwood area extended throughout the trunk, at least from the base to the crown (Fig. 2D, G). Type 2 trees displayed an irregular wetwood area that extended partly into the sapwood region (Fig. 2I), with a distribution pattern consistently observed at 8 m but not at 14 m height (Fig. 2C, F). Our X-ray scans further revealed that wetwood can extend vertically from the base to the crown in *Abies alba* trees and that observations made at the trunk base are representative of the overall state of the trunk.

Physical properties of wood (sapwood, heartwood, wetwood)

The moisture content of wetwood was consistently equal to, or higher, than that of sapwood, and significantly higher than in normal heartwood, as demonstrated by measurements in this study (Table 1, Figs. 3 and 4).

Regarding the hydraulic conductivity of the wood, our method indicated an average value of K of around 30 $mmol.m.s^{-1}.MPa^{-1}$ in the sapwood, but no conductivity in either wetwood or dry heartwood (Table 1).

The water retention curve of sapwood aligned with its susceptibility to cavitation, remaining constant at around 130% moisture content between + 0.5 and − 1 MPa before decreasing with the onset of cavitation, eventually reaching levels comparable to those of dry heartwood at around 40% from − 2.5 MPa (Fig. 3B). Wetwood's water retention curve differed greatly: between + 0.5 and − 1 MPa, a portion of the water is released, reducing the MC from 188 to 124% (a value close to that of sapwood at this point). However, unlike sapwood, pressure increase did not decrease wetwood's MC, which remained stable between 104 and 124% (Fig. 3B).

Under stable and controlled conditions, drying rates in both radial and longitudinal directions for sapwood and wetwood samples were identical (Fig. S2). Although the overall drying time was dependent on the initial MC, regardless of the wood type, a significant decrease in the drying time and rate of wetwood was observed when a zone of dry heartwood separated the wetwood from the outer zone (Fig. 4, Fig. S2).

Wetwood characteristics at the cellular level

We analyzed cores taken at breast height from 20 trees using X-ray microtomography to visualize the water content at the cellular level and distinguish between tracheids that were fully water-saturated (light grey areas) or embolized and filled with air (black areas). Figure 5a shows a typical radial pattern we observed in all trees containing wetwood areas. Three distinct zones were clearly visible: (1) In the sapwood (the first two rings on the left), X-ray microtomography revealed the alternation of almost entirely black areas corresponding to fully embolized tracheids in the latewood and light grey areas in the earlywood where almost all tracheids were saturated with water. This pattern was consistently observed in all sapwood rings of all trees studied. (2) The second zone, corresponding to the "dry" or "normal" heartwood, extended over about two rings and appeared completely black, consisting of fully embolized tracheids. Depending on the tree, the "dry" heartwood could extend several centimeters and never less than one ring (data not shown). (3) The wetwood present on the right side of Fig. 5A consisted of entirely light grey areas, indicating fully water-saturated xylem. This zone extended over a few growth rings in some trees and up to the entire heartwood in others. Depending on the tree, these light grey areas could contain black spots of varying sizes ranging from single tracheids to areas of several mm^2 filled with air.

At the anatomical level, we observed through light microscopy that all tori were aspirated in bordered pits in

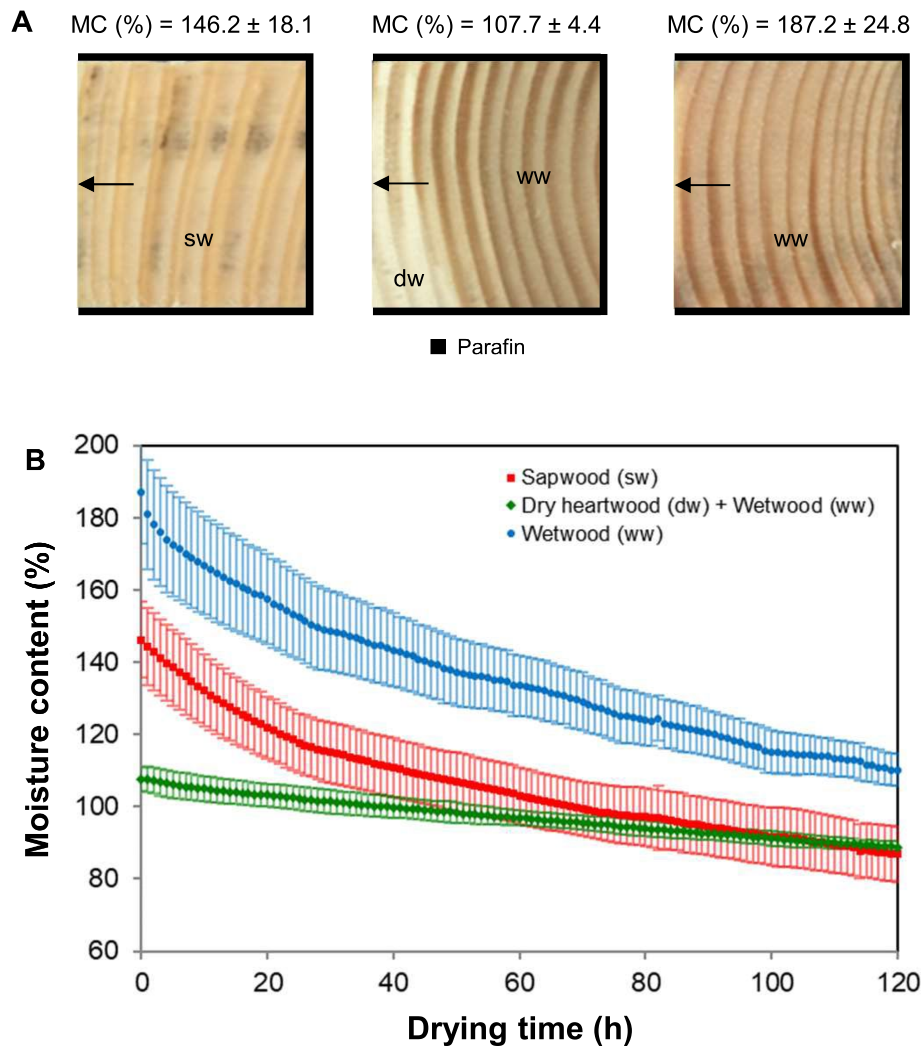

Fig. 4 Drying rate in radial direction of sapwood (sw), wetwood (ww) and wetwood separated from the outside by a dry heartwood zone (dw + ww) (**B**). Photographs depict the cross section of each type of wood samples. The black arrows indicate the drying direction (air/wood interface), while all other sides of the cube were watertight (**A**). Plot reports the mean MC values (± SD) during the drying

dry heartwood (Fig. 5C, F), while in the sapwood sections (Fig. 5B, E), no aspirated torus was observed. In the case of wetwood, all tori were aspirated in bordered pits of earlywood, which is a typical anatomical pattern of heartwood (Fig. 5D, G). Additionally, nuclei were present in every ray cell of the sapwood (Fig. 5B, E), but not visible in wetwood, which is another characteristic of heartwood (Fig. 5D, G).

Does wetwood have a physiological role?

To investigate fir trees' ability to mobilize the stored water in wetwood, we tracked the water status of a tree's aerial portion after removing its connection to the root system by girdling the sapwood (Fig. 7). Moisture content analysis of radial cores revealed that 90 days after girdling, the sapwood was completely dry, while the MC of the wetwood remained similar to its initial value at the time of girdling. At 650 days after the girdling, the fir tree's aerial part exhibited classic signs of apparent death (needle loss, bark stripping), but still retained high MC in its heartwood, albeit lower than before due to the presence of wetwood.

Discussion

Our measurements did not reveal any significant differences between the sites or among the trees within the same plot, indicating a lack of pronounced effects from pedoclimatic conditions.

Position of wetwood in the trunks

Our study revealed significant variations in water distribution in trunk heartwood, both horizontally and longitudinally, between the 3 felled trees. Similar variability has been observed previously in *Abies alba* (Martin et al. 2021) and in *Cryptomeria japonica* (Nakada et al. 2003). Contrary to several studies on *Abies* (Coutts and Rishbeth 1977; Passialis

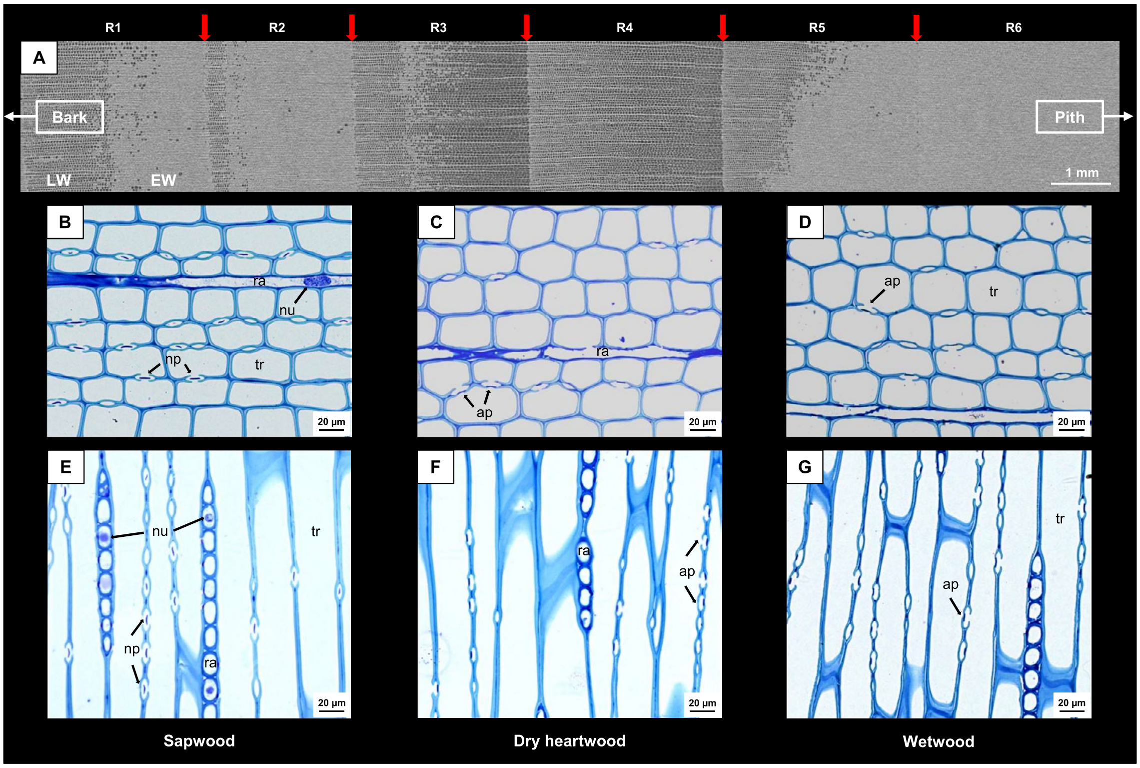

Fig. 5 X-ray microtomographic observation of tracheids embolism on cores (**A**). Black areas indicate air-filled tracheids, while light-grey areas indicate water-filled tracheids. The growth ring boundaries are indicated by red arrows.The directions of the bark and the pith are indicated by white arrows. EW, earlywood; LW, latewood. Scale bar: 1 mm. Anatomical structure of sapwood (**B**, **E**), dry heartwood (**C**, **F**) and wetwood (**D**, **G**) in transversal plane (**B**, **C**, **D**) and longitudinal plane (**E**, **F**, **G**). Staining: 1% toluidine blue. *Ap* aspirated pit, *np* non-aspirated pit, *nu* nucleus, *ra* ray cell, *tr* tracheid. Scale bar: 20 µm

and Tsoumis 1984), with the exception of one tree out of three, the wetwood does not show the typical pattern of a central circular cone starting from the base of the trunk and decreasing upwards (Fig. 2). In all the samples examined, we observed the presence of a dry zone of varying thickness between the sapwood and the wetwood (Figs. 2 and 5; Martin et al. 2021). The presence of such a zone has been reported in previous literature (Bauch et al. 1975; Worrall and Parmeter 1982). In a study on balsam fir, a transition zone of 1 to 2 rings between sapwood and wetwood was identified in 10 trees containing wet areas (Jeremic et al. 2004). The formation of this zone is believed to precede the formation of wetwood (Coutts and Rishbeth 1977).

Physical properties of wetwood

If the moisture content of heartwood exceeded the value of 50%, it was considered abnormal and identified as wetwood. On average, the moisture levels measured in the wetwood were equivalent to or slightly higher than those in the sapwood; supporting the findings of previous research on different fir species (Coutts and Rishbeth 1977; Jeremic et al. 2004; Lihra et al. 2000; Martin et al. 2021; Schneider and

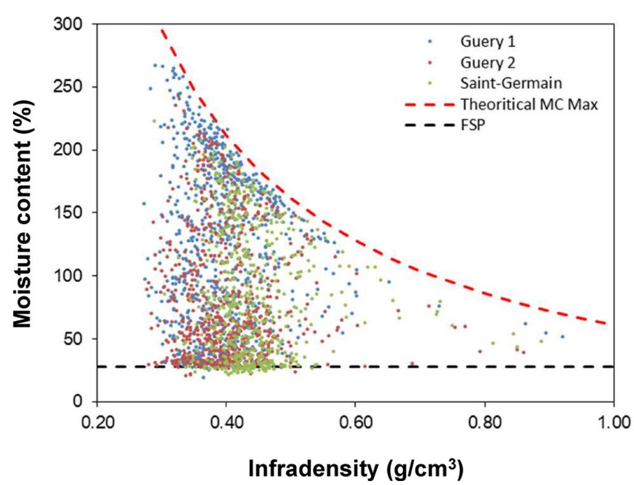

Fig. 6 Moisture content in relation to wood infradensity (see Eq. 3) of 2093 heartwood samples of approximatively 1 cm in length taken from 58 fir trees. The black dashed line indicates the FSP (Fibre Saturation Point) value. The red dashed curve indicates the theoretical maximum value the moisture content of wood could reach (see Eq. 4)

Zhou 1989; Worrall and Parmeter 1982). Figure 6 enlightens that no significant correlation was found between the presence of water in heartwood and wood density, which had already been observed in a study on Balsam fir (Jeremic et al. 2004). This graph also indicates that the moisture content in the trunk is always higher than the Fiber Saturation Point (FSP) value, even in case of normal "dry" heartwood, and can reach extremely high values; until the theoretical maximum value that is limited by the wood porosity, i.e. the wood density, according to the equation:

$$MC(\%)_{max} = 100\left(FSP + \rho_{water}\left(\frac{1}{\rho_W} - \frac{1}{\rho_{CW}}\right)\right) \quad (4)$$

where ρ_{CW} is the density of the cell wall (assumed to be constant: 1500 kg.m^{-3}, USDA 2010) and ρ_{Water} is the density of water. This observation suggests that there is no link between the presence of wetwood and tree growth rate as previously observed on *Abies balsamea* (Lihra et al. 2000). However, a study on *Abies grandis* showed a positive relationship between tree vigour and the proportion of wetwood in the tree (Coutts and Rishbeth 1977).

Longitudinally, wetwood shows no measurable conductivity under pressure (Table 1), with Fig. 3 highlighting the inability to push out water already present, even under pressure, suggesting a probably overall absence of water conduction, as observed for *Abies balsamea* and *Abies lasioscarpa* (Cai and Oliveira 2007; Schneider and Zhou 1989). This lack of conduction is attributed to the anatomical characteristics of the wetwood, notably bordered pits and dead ray cells (Schneider and Zhou 1989), suggesting that this wood has undergone a normal heartwood formation phenomenon characterized by embolism and cell death (Fig. 5). These results are consistent with water entry post-heartwood formation, rather than an initial defect in heartwood formation.

Regarding radial properties, our results show similar drying kinetics between sapwood and wetwood when the moisture content of the latter is relatively homogeneous (Figs. 4 and S2). However, a significant block seems to occur in the presence of a dry zone separating the wet zone from the surrounding air (Fig. 4). This observation is consistent with the work of Lihra et al. (2000) who proposed that drying problems in balsam fir may be due to blockage in some areas of the heartwood. In the presence of a dry zone, radial diffusion is very slow and requires prior water resaturation of the cell wall. This radial blockage due to the presence of a dry zone is confirmed by the presence of wetwood still visible in the heartwood of trees that have been dead for at least two years and have completely embolized sapwood (data not shown). Furthermore, girdling experiments demonstrated the absence or very low transfer of water from wetwood to sapwood, indicating no physiological role for this wood as a water reservoir (Fig. 7).

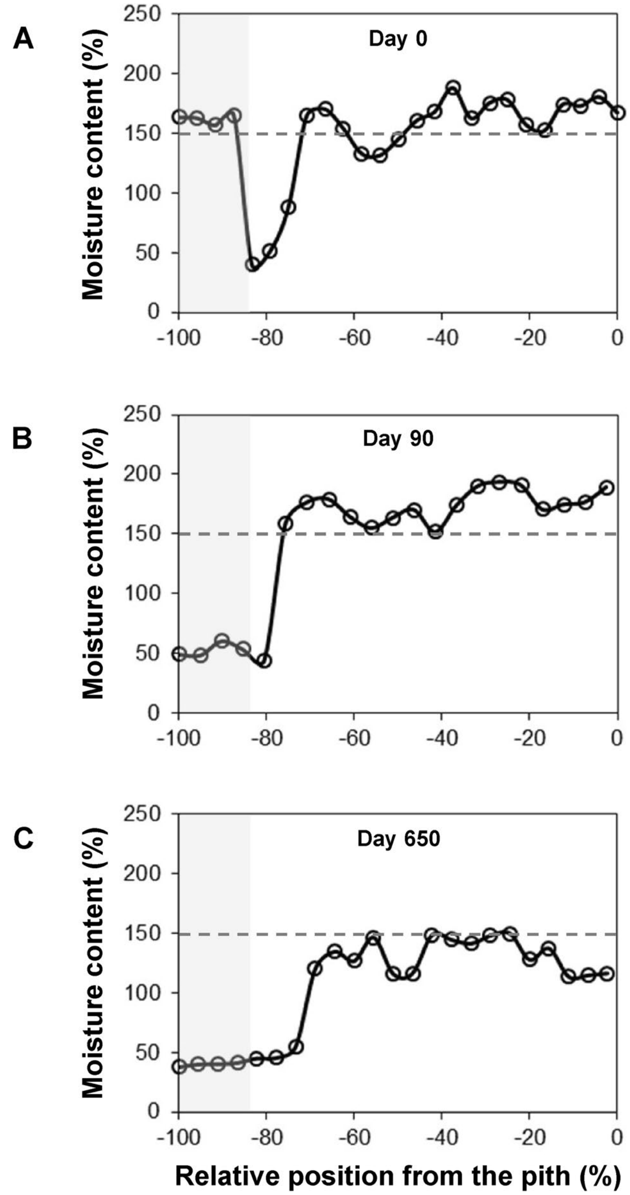

Fig. 7 Moisture content profiles in cores of a girdled tree: the day (**A**) of girdling (Day 0), 90 (**B**) and 650 (**C**) days after girdling (Day 90 and Day 650). On each profile, the sapwood area is highlighted in grey. Each point of the profiles corresponds to a 1 cm long radial core sample

Mechanism of wetwood formation

The mechanisms that facilitate water penetration into heartwood, despite the apparently impermeable barrier formed by the embolized zone that still separates sapwood from wetwood, have been the subject of a variety of studies (Coutts and Rishbeth 1977; Nakada et al. 2019; Okada et al. 2012; Worrall and Parmeter 1982).

A number of studies suggest that water entering the heartwood results from a transfer mechanism coming from the sapwood. In their study on *Abies grandis*, Coutts and Rishbeth (1977) claimed that the exclusive source of water comes from the sapwood through a movement of water through the few remaining viable woody rays in the transition zone. This transfer is facilitated by a difference in osmotic potential, attributed to an accumulation of potassium in the heartwood. Potassium accumulation in the heartwood has been linked to the development of wetwood in different species, including *Abies* (Ishii and Fukazawa 1987; Worrall and Parmeter 1982). In the case of *Cryptomeria japonica*, this accumulation would occur through an active transport by parenchyma cells of the rays just before their death during heartwood formation (Okada et al. 2012). The authors concluded that the accumulation of potassium and other alkali metals in Japanese cedar heartwood occurs in two phases: an active transport from the sapwood to the outer heartwood through the rays, followed by a diffusion within the heartwood. These processes appear to be independent of cambial activity and cytological changes in the ray parenchyma (Okada et al. 2012). In another study, a seasonally fluctuating osmotic potential gradient was demonstrated for the two species studied: *Cryptomeria japonica* and *Larix kaempferi*. Contrary to their initial hypothesis, the species lacking wetwood displayed the most pronounced gradient (Nakada et al. 2019). The transfer of water in the case of *Abies alba* appears to be less feasible, given that, in certain instances, there may be a dry wood layer exceeding 10 cm between the sapwood and the wetwood. (Fig. 2G; data not shown). Furthermore, a study carried out on three species, Douglas fir (*Pseudotsuga menziesii* Franco), ponderosa pine (*Pinus ponderosa* Dougl.) and lodgepole pine (*Pinus contorta* Dougl.) indicates that wood rays do not appear to facilitate radial water transport (Barnard et al. 2013).

In our study, an extensive examination of the distribution of wetwood in trunks (Figs. 2 and 8) enabled us to highlight the significant role played by dead branches in the wetwood formation process. Through X-ray scanner imaging, we observed that wetwood has the potential to extend vertically from the base of the trunk to the crown. (Fig. 2, Vid. S1). Eye observation of different wood sections revealed that the wetwood mainly established connections with dead branches (Fig. 8B, C), while living branches never showed a direct connection with wetwood (Fig. 8D). We therefore propose that the dead branches can act as a conduit, promoting the entry of external water and followed by mass diffusion into the heartwood around the dead branches in both radial and longitudinal directions; challenging the presumed impermeability of the heartwood, a phenomenon already suggested in other studies (Krause and Cagnon 2005; Worrall and Parmeter 1982). Our hypothesis is that filling could occur slowly and progressively over several years. This could be due to a diffusion of water along the cell walls, a diffusion that is lower than the resolution of the conductivity measurements carried out during our study. Occasionally, wetwood is also visible in the sapwood (Fig. 2F, I), in response or not to injury, but always as a result of tracheid embolism (data not shown).

In the case of softwoods, with a few rare exceptions, the development of wetwood appears to be a characteristic observed in species with wood lacking resin canals (Jeremic et al. 2004; Martin et al. 2021; Nakada et al. 2003; Nakada 2006; Passialis and Tsoumis 1984; Ward and Pong 1980). The presence of these canals may consequently account for the absence of wetwood in certain species such as *Larix kaempferi*, despite exhibiting a more significant osmotic gradient than *Cryptomeria japonica* (Nakada et al. 2019). By making perforations in the bark and sapwood of several living *Abies alba* and *Picea abies* trees, we observed, two years later, the formation of wetwood areas in the sapwood region of the *Abies alba* trees, extending a minimum of 10 cm above and below the perforation site. In contrast, *Picea abies* trees only showed embolization of their sapwood at equivalent distances from the perforations (data not shown). This distinction could be attributed to the presence of resin canals and production of resin in response to wounding in *Picea abies* trees.

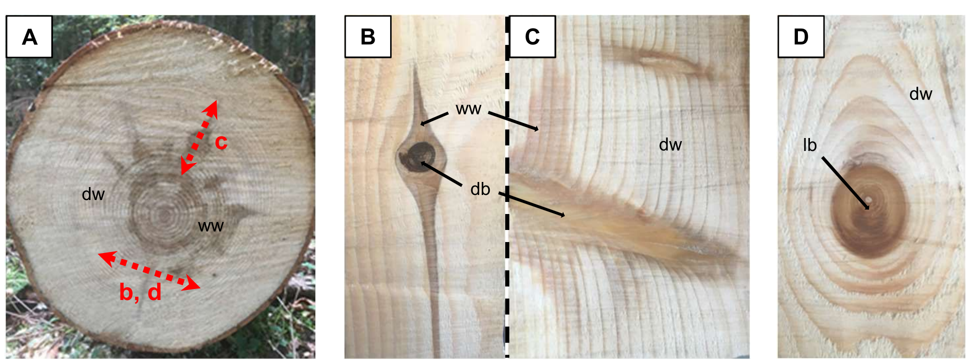

Fig. 8 Pattern of wetwood in transverse section of a felled tree (**A**). Water diffusion zones (ww) around dead branches (db) observable on longitudinal-tangential (**B** and **D**) and longitudinal-radial sections (**C**). There is never wetwood around living branches. db: dead branch; dw: dry wood; lb: leaving branch; ww: wetwood

Conclusion

This article presents a number of significant findings, which are outlined below: (1) the pronounced variability of moisture distribution in the heartwood of the silver fir trees examined, which revealed the absence of a predetermined pattern; (2) the distinct divergence in physical properties between wetwood and sapwood, in particular the zero hydraulic conductivity of wetwood; and (3) the identical anatomical characteristics of wetwood compared to normal dry heartwood. In regard to the potential role of water in fir heartwood, two main hypotheses have been proposed in the literature. The first posits that stored water may have a physiological function that has yet to be conclusively demonstrated. The second suggests that the formation of wetwood may be the consequence of a defect or anomaly resulting from a difference in osmotic potential, leading to an accumulation of water in the heartwood. In this work, we have demonstrated that wetwood is unable to provide a water reserve for the tree, given its compartmentalized and apparently non-usable nature. The potential protective role against bacteria and fungi could be a plausible assumption, especially considering the prevalence of water in the heartwood of *Abies alba* as a species lacking resin canals. However, further research is required to confirm or refute this hypothesis. In addition, our work has highlighted the crucial role of dead branches in the mechanism of wetwood formation in silver fir. Finally, with regard to the challenges associated with the use of fir wood in industry, it should be noted that the presence of water in the heartwood has a negligible impact on the wood's intrinsic quality. However, this can potentially affect the processing of the wood, for example, by affecting the effectiveness of drying, steaming or gluing.

Supplementary Information The online version contains supplementary material available at https://doi.org/10.1007/s00468-024-02575-w.

Acknowledgements The authors are grateful to the French National Forestry Office (ONF) and the French National Center for Forest Ownership (CNPF) for their help in finding experimental sites. The authors would also like to thank SILVATECH (Silvatech, INRAE, 2018. Structural and functional analysis of tree and wood facility, https://doi.org/10.15454/1.5572400113627854E12) for the X-ray CT scanning of the logs.

Author contribution statement Ludovic Martin, Nicole Brunel-Michac, Pierre Conchon, Hervé Cochard, Eric Badel. Conception and design: Ludovic Martin, Hervé Cochard, Eric Badel. Methodology implementation: Ludovic Martin. Experiment execution: Ludovic Martin, Nicole Brunel-Michac, Pierre Conchon. Data collection: Ludovic Martin. Data analysis/interpretation: Ludovic MARTIN, Hervé Cochard, Eric Badel. Manuscript writing/revision: Ludovic Martin, Hervé Cochard, Eric Badel.

Funding This study was part of the Sap-In project AV0014860 funded by the European Regional Development Fund (ERDF) within the framework of the ERDF/ESF Auvergne operational program for the 2014–2020 programming period.

Data and materials availability The datasets generated during and/or analysed during the current study are available from the corresponding author on reasonable request.

Declarations

Conflict of interest The authors have no relevant financial or non-financial interests to disclose.

References

Azri W, Chambon C, Herbette S, Brunel N, Coutand C, Leple JC, Ben Rejeb I, Ammar S, Julien JL, Roeckel-Drevet P (2009) Proteome analysis of apical and basal regions of poplar stems under gravitropic stimulation. Physiol Plant 136:193–208. https://doi.org/10.1111/j.1399-3054.2009.01230.x

Barnard DM, Lachenbruch B, McCulloh KA, Kitin P, Meinzer FC (2013) Do ray cells provide a pathway for radial water movement in the stems of conifer trees. Am J Bot 100(2):322–331. https://doi.org/10.3732/ajb.1200333

Bauch J, Höll W, Endeward R (1975) Some aspects of wetwood formation in fir. Holzforschung 29(6):198–205

Billon LM, Blackman CJ, Cochard H, Badel E, Hitmi A, Cartailler J, Souchal R, Torres-Ruiz JM (2020) The droughtbox: a new tool for phenotyping residual branch conductance and its temperature dependence during drought. Plant, Cell Environ 43:1584–1594. https://doi.org/10.1111/pce.13750

Cai L, Oliveira LC (2007) Gas permeability of wetwood and normal wood of subalpine fir in relation to drying. Drying Technol 25:501–505. https://doi.org/10.1080/07373930601184072

Cochard H, Damour G, Bodet C, Tharwat I, Poirier M, Ameglio T (2005) Evaluation of a new centrifuge technique for rapid generation of xylem vulnerability curves. Physiol Plant 124:410–418. https://doi.org/10.1111/j.13999-3054.2005.00526.x

Cochard H, Badel E, Herbette S, Delzon S, Choat B, Jansen S (2013) Methods for measuring plant vulnerability to cavitation: a critical review. J Exp Bot 64(15):4779–4791. https://doi.org/10.1093/jxb/ert193

Cochard H, Delzon S, Badel E (2015) X-ray microtomography (micro-CT): a reference technology for high-resolution quantification of xylem embolism in trees. Plant, Cell Environ 38:201–206. https://doi.org/10.1111/pce.12391

Coleman JS, Murdoch CW, Campana RJ, Smith WH (1985) Decay resistance of elm wetwood. Can J Plant Path 7(2):151–154. https://doi.org/10.1080/07060668509501492

Coutts MP, Rishbeth J (1977) The formation of wetwood in grand fir. Eur J Forest Pathol 7:13–22

Etheridge DE, Morin LA (1962) Wetwood formation in balsam fir. Can J Bot 40:1335–1345

Ishii T, Fukazawa K (1987) Sap constituents and pit closures connected with water penetration in the wetwood of Abies sachalinensis Masters. Res Bull Coll Exp for Hokkaido Univ 44:1277–1305

Jeremic D, Cooper P, Srinivasan U (2004) Comparative analysis of balsam fir wetwood, heartwood, and sapwood properties. Can J for Res 34:1241–1250. https://doi.org/10.1139/x03-287

Krause C, Gagnon R (2005) Wet heartwood distribution in the stem, stump, and root wood of black spruce in the quebec boreal forest, Canada. North J Appl for 22:12–18. https://doi.org/10.1093/njaf/22.1.12

Krause C, Gagnon R (2006) The relationship between site and tree characteristics and the presence of wet heartwood in black spruce in the boreal forest of quebec, Canada. Can J for Res 36:1519–1526. https://doi.org/10.1139/x06-026

Lihra T, Cloutier A, Zhang SY (2000) Longitudinal and transverse permeability of balsam fir wetwood and normal heartwood. Wood Fiber Sci 32:164–178

Mackay JFK (1975) Properties of northern aspen discoloured wood related to drying problems. Wood and Fiber 6(4):319–326

Martin L, Cochard H, Mayr S, Badel E (2021) Using electrical resistivity tomography to detect wetwood and estimate moisture content in silver fir (Abies alba Mill.). Annals Forest Sci. https://doi.org/10.1007/s13595-021-01078-9

Moya R, Munoz F, Jeremic D, Berrocal A (2009) Visual identification, physical properties, ash composition, and water diffusion of wetwood in *Gmelina arborea*. Can J for Res 39:537–545. https://doi.org/10.1139/X08-193

Nakada R (2006) Within-stem water distribution in living trees of some conifers. IAWA J 27:313–327

Nakada R, Fujisawa Y, Yamashita K, Hirakawa Y (2003) Changes in water distribution in heartwood along stem axes in *Cryptomeria japonica*. J Wood Sci 49:107–115. https://doi.org/10.1007/s100860300017

Nakada R, Okada N, Nakai T, Kuroda K, Nagai S (2019) Water potential gradient between sapwood and heartwood as a driving force in water accumulation in wetwood in conifers. Wood Sci Technol 53:407–424. https://doi.org/10.1007/s00226-019-01081-4

Okada N, Hirakawa Y, Katayama Y (2012) Radial movement of sapwood-injected rubidium into heartwood of Japanese cedar (*Cryptomeria japonica*) in the growing period. J Wood Sci 58:1–8. https://doi.org/10.1007/s10086-011-1218-6

Passialis C, Tsoumis G (1984) Characteristics of discoloured and wetwood in fir. IAWA Bulletin 5(2):111–120

Schink B, Ward JC (1984) Microaerobic and anaerobic bacterial activities involved in formation of wetwood and discoloured wood. IAWA J 5(2):105–109. https://doi.org/10.1163/22941932-90000872

Schneider MH, Zhou L (1989) Characterization of wetwood from 4 balsam fir trees. Wood Fiber Sci 21:1–16

Sperry JS, Donnelly JR, Tyree MT (1988) A method for measuring hydraulic conductivity and embolism in xylem. Plant Cell and Environnement 11:35–40. https://doi.org/10.1111/j.1365-3040.1988.tb01774.x

USDA (2010) Wood Handbook: Wood as an Engineering Material. U.S. Dept. of Agriculture, Forest Service, Forest Products Laboratory, Madison, WI

Van der Kamp BJ, Gokhale AA, Smith RS (1979) Decay resistance owing to near-anaerobic conditions in black cottonwood wetwood. Can J for Res 9(1):39–44. https://doi.org/10.1139/x79-007

Ward JC (1984) Influence of wetwood on pulsed-current resistance in lumber before and during kiln-drying. Wood Fiber Sci 16(4):598–617

Ward JC (1985) The effect of wetwood on lumber drying times and rates: an exploratory evaluation with longitudinal gas permeability. Wood Fiber Sci 18(2):288–307

Ward JC, Pong WY (1980) Wetwood in trees: a timber resource problem. USDA Forest Service General Technical Report PNW 112, USDA Forest Service Pacific Northwest Forest and Range Experimental Station.

Ward JC, Zeikus JG (1980) Bacteriological, chemical and physical properties of wetwood in living trees. In Natural variations of wetwood in living properties. Edited by J. Bauch. Mitt. Bundesforschungsanst. Forst Holzwirtsch. No. 131. pp. 133-165

Wilcox WW (1968) Some physical and mechanical properties of wetwood in white fir. For Prod J 18(12):27–31

Worrall JJ, Parmeter JR (1982) Formation and properties of wetwood in white fir. Phytopathology 72:1209–1212. https://doi.org/10.1094/Phyto-77-1209

Xu Z, Leininger TD, Lee AWC, Tainter FH (2001) Chemical properties associated with bacterial wetwood in red oaks. Wood Fiber Sci 33(1):76–83